A Mechanistic Study of Wettability Alterations in Sandstone by Low Salinity Water Injection (LSWI) and CO_2 Low Salinity Water-Alternating-Gas (WAG) Injection

Shijia Ma[1] and *L.A.* James[1,*]

[1]Hibernia EOR Research Group, Department of Process Engineering, Memorial University of Newfoundland, St. John's, NL, Canada, A1B 3X5

Abstract. Low salinity water injection (LSWI), an emerging Enhanced Oil Recovery (EOR) method, has proven to be effective in increasing oil recovery by wettability alteration. As low salinity water is injected into the reservoir, the pre-established equilibrium is disturbed. The chemical reactions among the oil/brine/rock system alters the existing wettability, resulting in enhanced oil recovery. Water-alternating-gas (WAG) injection is also a leading EOR flooding process in light to medium oil sandstone and carbonate reservoirs. A recently proposed hybrid EOR method, CO_2 low salinity (LS) WAG injection, shows promise based on experimental and simulation studies, compared to LSWI or CO_2 injection alone. Wettability alteration is considered as the dominant mechanism for CO_2 LSWAG injection. In this study, a new displacement contact angle measurement which better mimics the actual displacement process taking place in a reservoir is used, aiming to investigate the effect of monovalent and divalent cations, CO_2, and injection schemes. It is found that the injection of NaCl low salinity water alters the wettability towards slightly water-wet, and the injection of $CaCl_2$ low salinity water alters the wettability towards slightly oil-wet. The injection of CO_2 promotes water-wetness and geochemical reactions between oil and brine. Injection scheme of CO_2 and NaCl low salinity water is more efficient than WAG cycle of CO_2/NaCl in wettability alteration towards more water-wet. However, the opposite trend is observed with $CaCl_2$ low salinity water, of which WAG cycle of CO_2/$CaCl_2$ is more efficient in altering wettability towards water-wet. The oil drop deformation process during LSWI resembles the process of oil removal using surfactant. As CO_2 is introduced, due to the acidic effect of CO_2 and ion exchange, it acts to wet the rock surface, leading to a more water-wet state. With introduction of CO_2, the oil drop deformation resembles the "roll-up" oil removal process.

1 Introduction

Low salinity water injection (LSWI) has been widely investigated and recognized as an effective enhanced oil recovery (EOR) method in both secondary and tertiary mode [1-3]. Compared to other chemical EOR methods, such as polymer or surfactant flooding, LSWI is advantageous due to its lower cost and reduced impact on the environment. Another advantage for LSWI is that it can be combined with other EOR methods to further improve oil recovery [4-6]. According to economic evaluations on chemical EOR methods by Al-Murayri et al. [7] and Muriel et al. [8], LSWI and CO_2 injection generate the highest net present value (NPV) and both methods are effective in increasing oil recovery. Therefore, a hybrid technique termed CO_2 low salinity water-alternating-gas (LSWAG) injection, which combines the EOR effect of both methods, has been developed over the last 15 years. CO_2 LSWAG injection has been studied through core flooding experiments, contact angle and interfacial tension (IFT) measurements, primarily with sandstone, at ambient or reservoir conditions. Most results confirm improved oil recovery using this hybrid technique, in both secondary and tertiary modes, with some exceptions [9-11]. Studies with negative or neutral outcomes are mainly due to the fact that the cores are strongly water-wet or contain very small amount of clay minerals. Clean water-wet sandstones may not be the most favourable reservoir conditions for CO_2 LSWAG injection [12, 13].

The proposed mechanisms of CO_2 LSWAG injection are a combination of LSWI and CO_2 WAG injection. Al-Abri et al. [14] proposed that the improved oil recovery by immiscible CO_2 LSWAG injection is due to mobility control and wettability alteration. The IFT between high salinity brine and oil reduces as CO_2 is introduced. However, changes in the IFT of low salinity brine and oil are not noticeable, indicating that IFT reduction is not a dominant mechanism in this process. They also suggest multi-component ionic exchange (MIE) in which Na^+ substitutes the divalent cations (Mg^{2+}) accounts for the higher oil recovery when injecting monovalent NaCl brine compared to injection of $MgCl_2$ brine. Teklu et al. [15] claimed that CO_2 LSWAG injection improved oil recovery of conventional CO_2 WAG injection by forming in-situ carbonated water of higher CO_2 saturation in the brine phase due to the higher CO_2 solubility in low salinity water. This in-situ carbonated water promotes wettability alteration towards more water-wet and CO_2-brine IFT reduction, hence improved oil recovery. They also compared the CO_2-brine solubility model developed by Enick and Klara [16] and Li and Nghiem [17] with fresh water and

* Corresponding author: ljames@mun.ca

100,000 ppm NaCl at 71ºC from 0 to 41 MPa. Both models show that CO_2 solubility in brine increases with pressure and CO_2 solubility is higher in fresh water. Chaturvedi et al. [18] and AlQuraishi et al. [11] suggest that fines migration and wettability alteration, mechanisms of LSWI, might be the dominant mechanisms for increased oil recovery by CO_2 LSWAG injection. The presence of clay minerals, especially kaolinite, is considered essential. However, this proposed mechanism is questioned by Zolfaghari et al. [19] as they achieved oil recovery in sandstone without kaolinite. Wettability alteration towards more water-wet was suggested by Al-Saedi et al. [20-22]. Based on the proposed mechanisms, wettability alteration and mobility control may be considered as the dominant mechanisms in CO_2 LSWAG injection.

Wettability alteration taking place during CO_2 LSWAG injection could be ascribed to LSWI or the acidic effect of CO_2 [23, 24] or a combination of both. Drummond and Israelachvili [25] demonstrate wettability alteration, indicated by contact angle measurements at ambient conditions for low salinity water, varying from oil-wet to water-wet as pH is lower than 9 and from water-wet to intermediate-wet as pH is greater than 9. The pH during a LSWI is mostly below 9 [26], indicating the wettability alteration is more likely to be from water-wet to intermediate-wet [27]. The main functions of injecting CO_2 are oil swelling, viscosity reduction due to CO_2 solubility in oil, miscibility with oil if pressure is above minimum miscible pressure and wettability modification [21]. Since low salinity water and CO_2 both impact wettability, the question remains as to whether the introduction of CO_2 in low salinity water will assist in promoting the geochemical reactions and low salinity effect. Generally, monovalent cations (Na^+) and divalent cations (Ca^{2+} or Mg^{2+}) have different impacts on the rock surface. The MIE mechanism by LSWI proposed by Lager et al. [28] demonstrates that multivalent cations, such as Ca^{2+}, act as bridges between the oil polar components and the negatively charged rock surface, promoting oil-wetness. The mechanism of electrical double layer expansion by LSWI suggested by Ligthelm et al. [29] indicates that lowering the electrolyte content, especially reducing the content of multivalent cations, yields expansion of the electrical double layer surrounding the clay and oil, and an increase in zeta potential. This leads to wettability modification of the rock surface towards more water-wet. Wettability characterization is uncertain for CO_2 introduced with low salinity water in the sandstone/oil/brine/rock system since previous experimental data is limited.

To investigate wettability of the rock and fluid systems, direct or indirect and qualitative or quantitative methods can be used. Indirect and qualitative methods for characterizing rock wettability are capillarimetric method [30], spontaneous imbibition [31, 32], capillary pressure curves, and relative permeability method [33, 34]. Indirect and quantitative methods include the Amott and Amott-Harvey index method, USBM (U.S. Bureau of Mines) method, and the combined Amott/USBM method, which measure the average wettability of the rock samples, i.e., a macroscopic mean value of the rock wettability to a given fluid. Direct and quantitative method for characterizing the wettability of a specific surface is the contact angle measurement [35, 36], as well as the new SEM-MLA method introduced [37, 38]. Contact angle measurement works the best with pure fluids and well-prepared surfaces [39]. It can also be used to determine the effect of crude oil, brine chemistry, temperature and pressure on wettability. According to Arif et al. [40], direct contact angle measurement is a widely recognized technique for wettability characterization of rock/CO_2/brine or rock/oil/CO_2-enriched-brine systems. In this research we used contact angle measurement as a method to evaluate wettability alteration. Our particular interest is understanding the ion exchange and chemical reactions of the rock/oil/brine/ and rock/oil/brine/CO_2 systems by comparing the effect of monovalent and divalent ions and the effect of CO_2 on water-wet and oil-wet sandstone under different injection sequences. Contact angle measurements may indeed be the best choice to differentiate any wettability changes as we are able to 1) conduct measurements with high temperature and pressure, under which the commonly used Amott or USBM method is not applicable [40, 41] and 2) still appreciate the core scale aspects of rock mineralogy and some differences in water-wet and oil-wet "real" surfaces [42].

The data for contact angle measurements on sandstone/crude oil/CO_2-enriched brine system is very limited. Jaeger et al. [43] performed captive bubble contact angle measurements with sandstone samples which were previously aged at room temperature with 1.5 wt% cyclohexanepentanoic acid in decane for two months. They reported a strongly water-wet condition, contact angle of 46º, of such system under 50ºC and 20.7 MPa with 32,000 ppm synthetic seawater. Ameri et al. [44] conducted contact angle measurements on Bentheimer sandstones that are initially water-wet and oil-wet at elevated pressure from 0.2 to 14 MPa and with NaCl brine salinity ranging from 5000 to 35,000 ppm. They found that in initially water-wet sandstones, contact angle increases with pressure, and decreases with increasing NaCl brine concentration. The overall contact angle for using NaCl brine salinity ranging from 20,000 to 35,000 ppm is very low, less than 20º. The average contact angle for using 5000 ppm NaCl brine is 40º and the value when distilled water is used is 57º. This indicates that decreasing salinity of NaCl brine leads to a less water-wet state, which differs from the results obtained by Espinoza et al [45]. For initially oil-wet sandstone, samples were aged for 22 months with crude oil at 60ºC. In the sub-critical and near-critial state region of CO_2 (0-9 MPa), contact angle increase is slightly higher with 35,000 ppm brine than with distilled water. However, the opposite is observed for super-critical state region of CO_2 (9-13 MPa), Seyyedi et al. [46] reported that contact angle values of the quartz with CO_2-enriched brine are slightly higher than that with brine phase alone, indicating that injection of CO_2 alters wettability towards slightly less water-wet. However, Al-Abri et al. [14] reported contradictory results, showing that the contact angle was reduced with the addition of CO_2, indicating a wettability alteration towards more water-wet. They conducted their contact angle measurements with Berea sandstone discs aged with crude oil at 60º for three weeks. They also found that changes in wettability are greater with divalent ions (Mg^{2+}) than monovalent ions (Na^+ and K^+).

It is worth mentioning that there are limitations on these contact angle measurements that would result in misleading interpretations on the effect of CO_2 and low salinity water, and the working mechanisms of CO_2 LSWAG injection. In

these measurements, the oil drop is introduced after the rock surface has been in contact with injection brine and CO_2, which is not representative of the actual displacement in a reservoir, where oil exists before the injection fluids. Therefore, in order to better capture and mimic the real displacement procedure taking place in a reservoir to investigate what triggers the wettability alteration during LSWI and CO_2 LSWAG injection, a displacement method developed by Sofla et al. [42] for measuring contact angle was employed in this study. We investigated the dynamic contact angle changes during the displacement process of LSWI, continuous CO_2 and LSWI, and CO_2 LSWAG injection, respectively. With this method, the interactions among crude oil, brine and CO_2 were investigated without the additional effect of capillary imbibition and drainage [47]. The objective is to compare the resulting wettability alteration (through contact angle measurements) due to multi-component ion exchange (MIE), chemical reactions, and injection sequence of low salinity water. This paper addresses the question as to whether or not the ionic charge and injection scheme play a role in differentiating LSWI and CO_2 LSWAG injection at the fluid-rock interaction level.

2 Materials

Fluids. The oil phase used in this experiment is an offshore Newfoundland and Labrador (NL) light crude oil. Synthetic brines were prepared to mimic the Hibernia formation water and Grand Banks seawater. The two low salinity brines are 2000 mg/L NaCl and 2000 mg/L $CaCl_2$. Their chemical compositions and basic properties are presented in Table 1.

Table 1. Compositions and properties of synthetic brines and oil

Component	FB	SW	NaCl	$CaCl_2$
Na^+, mg/L	35,671	10,974	786	/
Mg^{2+}, mg/L	330	1,310	/	/
Ca^{2+}, mg/L	3,599	420	/	721
K^+, mg/L	255	407	/	/
Cl^-, mg/L	62,371	19,740	1,214	1,279
SO_4^{2-}, mg/L	233	2,766	/	/
HCO_3^-, mg/L	/	129	/	/
Total	**102,430**	**35,746**	**2,000**	**2,000**
pH@22° C	5.9	7.9	6.2	5.8
Density, g/cm³	1.074	1.023	1.0	1.0
Oil Viscosity, cP	5.0			
Oil Density, g/cm³	0.878			

Legends: FB – formation brine; SW – seawater; / - not included

Rock sample. Berea sandstone with 80% quartz content and <2% clay content [37] was used in this study. The core samples with an approximate diameter of 2 cm were cut into 5-mm thin slices using MK-370EXP Tile Saw. The dust was blown off with pressurized nitrogen and the core slices were dried in oven overnight. The water-wet samples were immersed in formation brine for one day prior to conducting contact angle measurements. To obtain an oil-wet initial wettability, the core slices initially immersed in formation brine were removed to a beaker containing NL crude oil and aged at 98ºC in the oven for six weeks as suggested by Sripal et al. [37] to obtain oil-wet conditions. Subsequently, the surface of the oil-wet samples was cleaned and immersed in formation water for one day before contact angle measurements.

3 Methods

Figure 1 illustrates the experimental setup used to perform contact angle measurements in this study. All experiments are conducted at ambient conditions. In order to mimic the actual displacement taking place in a reservoir, the cell is initially filled with formation brine. Subsequently, an oil drop with radius ranging from 1.8 to 2.0 mm is introduced through the needle at the bottom of the cell and adheres onto the rock surface. The initial contact angles are measured after the system reached equilibrium, which is 1 hour after the oil drop was introduced into the system. This indicates the initial wettability of the rock surface and initial condition of an oil droplet in a reservoir.

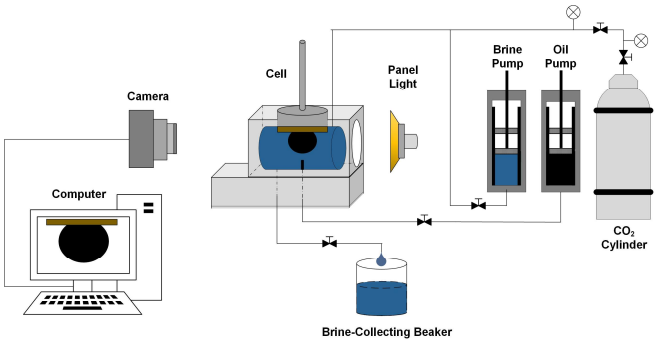

Fig. 1 Schematic diagram of contact angle measurement.

A total of 13 experiments were completed, using the injection schemes outlined in Table 2. Each scenario was completed twice, once using NaCl as the LSW and again using $CaCl_2$ as the LSW.

Table 2. Injection scheme of experiments

Scenario #	Injection Scheme			
	Cycle 1 (60 mL)	Cycle 2 (20 mL)	Cycle 3 (20 mL)	Cycle 4 (20 mL)
1	SW	SW	SW	SW
2	SW	LSW	LSW	LSW
3	LSW	LSW	LSW	LSW
4	SW	CO_2 (10ml)	LSW (25mL)	LSW (25mL)
5	SW	CO_2/LSW	CO_2/LSW	CO_2/LSW
6	LSW	CO_2 (10mL)	LSW (25mL)	LSW (25mL)
7	LSW	CO_2/LSW	CO_2/LSW	CO_2/LSW

Scenario #1 represents seawater injection. Scenario #2 and #3 represent LSWI. Scenarios #4 and #6 represents seawater or low salinity water injection, followed by continuous CO_2 injection and LSWI. Scenario #5 and #7 represent seawater or low salinity water injection, followed

by LSWAG injection. Brines and CO_2 are injected through the injection inlet into the cell to displace the existing fluid. The injection speed is controlled so that the oil drop remains attached on the rock surface throughout the experiment.

The total volume of the cell is 20 mL. In cycle 1, 60 mL of seawater or low salinity water is injected to ensure that the initial formation brine is fully displaced. The system is allowed to set for equilibrium for half an hour after every 20 mL of injection fluid and the reading at equilibrium state is taken. Figure 2, as an example, shows the contact angle changes during the half-an-hour equilibrium time of scenario #1, indicating that an equilibrium was gradually established.

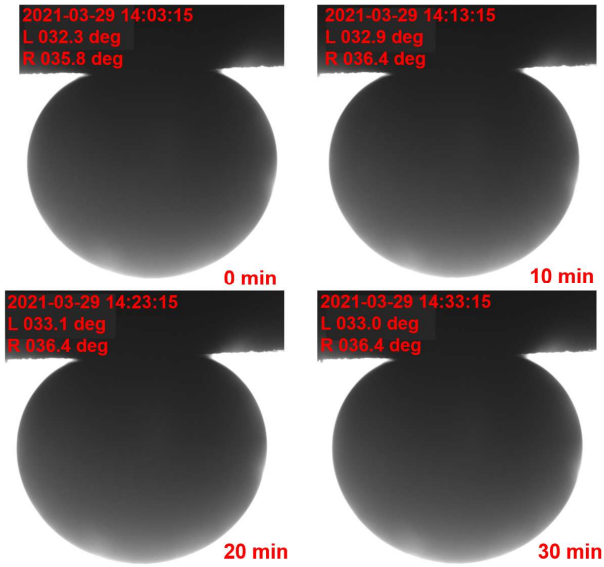

Fig. 2 Contact angle changes after seawater injection during half-an-hour equilibrium time (scenario #1).

After cycle 1, another 60 mL of CO_2 (g), low salinity water and a combination of both are further injected in cycles 2-4 representing the injection schemes of continuous CO_2 and low salinity water injection, and the CO_2 LSWAG process. Contact angles are measured dynamically for each injection cycle and measurements are taken half an hour after each injection cycle. Three distinct measurements are carried out to monitor repeatability. Contact angles are reported as averages of the three measurements. The change in contact angle is calculated using the equation below.

$$\Delta\theta\ [\%] = (\theta - \theta_{initial})/\theta_{initial} \times 100 \qquad (1)$$

where $\Delta\theta$ refers to the change in contact angle, θ is the value of contact angle measured after each injection cycle, and $\theta_{initial}$ is the initial contact angle measured with the presence of formation water. The reason for comparing changes instead of absolute contact angles is to avoid the influence of the samples and each scenario starts from the same point. Initial contact angle is also reported.

To calculate the uncertainty, or error propagation of $\Delta\theta$, the root-sum square method proposed by Kline and McClintock is used [48]. The effect of uncertainty $\sigma_{\Delta\theta}$ on the calculated $\Delta\theta$ can be expressed as follow:

$$\sigma_{\Delta\theta} = \sqrt{\sigma_{\theta}^2 * (\frac{\partial(\Delta\theta)}{\partial\theta})^2 + \sigma_{\theta_{initial}}^2 * (\frac{\partial(\Delta\theta)}{\partial\theta_{initial}})^2} \quad (2)$$

Subsequently, changes in contact angle with calculated uncertainty are plotted against injected volume to investigate the effect of low salinity water, injection of CO_2 and WAG injection schemes.

Moreover, in order to validate that the measured contact angle changes are mainly due to the chemical reactions (intermolecular forces) in the oil/brine/rock system, rather than gravitational force, we have estimated the Bond number (B_o) of the oil/seawater/brine system using equation from Li et al. [49].

$$B_o = \frac{\Delta\rho g L^2}{\gamma} \qquad (3)$$

where $\Delta\rho$ is the density difference of oil and brine (kg/m^3), g is gravitational acceleration (m/s^2), L refers to the radius of curvature of oil drop (m), γ is surface tension (N/m). With the measured surface tension (31.5 mN/m), and oil drop radius in seawater (1.86 mm), Bond number is calculated to be 0.154, which is lower than 1, indicating that surface tension dominates.

4 Results and Discussion

As shown in Table 3, section 4.1 investigates the effect of seawater and low salinity water (scenario #1, #2 and #3) on wettability alteration of water-wet and oil-wet Berea sandstone samples. Section 4.2 discusses the effect of CO_2 by comparing scenario #2 and #4, and #3 and #6. Subsequently, the deformation process of the oil drops during the injection of low salinity water and CO_2 is investigated in section 4.3. In the end, section 4.4 studies the effect of different injection schemes by comparing CO_2 + LSW injection scheme to CO_2/LS WAG injection scheme (#4 and #5, and #6 and #7). The effect of monovalent and divalent cations is discussed and compared in all sections.

Table 3. Comparison of different scenarios.

Section	Comparison of different scenarios	
4.1 Effect of Low Salinity Water	#1	SW + SW
	#2	SW + LSW (NaCl and $CaCl_2$)
	#3	LSW + LSW (NaCl and $CaCl_2$)
4.2 Effect of CO_2	#2	SW + LSW
	#4	SW + CO_2 + LSW
	#3	LSW + LSW
	#6	LSW + CO_2 + LSW
4.4 Effect of Injection Scheme	#4	SW + CO_2 + LSW
	#5	SW + CO_2/LS WAG
	#6	LSW + CO_2 + LSW
	#7	LSW + CO_2/LS WAG

4.1 Effect of Low Salinity Water

Contact angle changes due to the injection of seawater alone, low salinity waters alone, and combinations of seawater and low salinity water are shown in Figures 3 and 4 for water-wet and oil-wet sandstones, respectively. These injection schemes mimic the displacement process of (1) seawater injection, (2) secondary seawater and tertiary LSWI, and (3) LSWI. Overall, changes in contact angle in the oil-wet samples are not as significant as in water-wet samples. However, it is

worth comparing and understand the changing trend after each injection cycle, which could be an estimation for the potential changes in a core scale experiment.

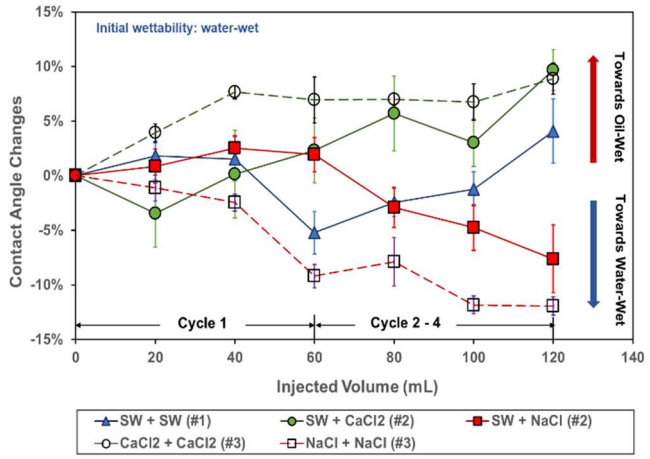

Fig. 3 Contact angle changes during seawater and low salinity water injection in water-wet sandstone (scenario #1, #2, #3).

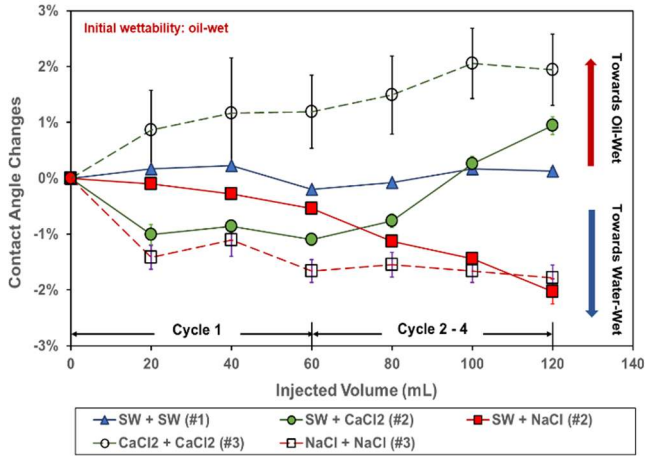

Fig. 4 Contact angle changes during seawater and low salinity water injection in oil-wet sandstone (scenario #1, #2, #3).

In Figure 3, the initial wettability of the rock sample is water-wet, with measured contact angles varying from 34º to 50º (average: 40.6º±5.0º). Contact angle changes due to the injection of seawater are within 5%, which is not very significant. This indicates that the injection of seawater has negligible effect on the rock wettability. The trend of using NaCl and $CaCl_2$ in LSWI shows different impacts on wettability. The red arrow in Figure 2 indicates changing towards more oil-wet and the blue arrow suggests changing towards more water-wet. It is seen that NaCl alters the wettability towards more water-wet, around 10% less compared to initial contact angle, whereas $CaCl_2$ results in wettability alteration moving to less water-wet. A similar trend is also observed in the combined seawater and LSWI process.

In Figure 4, the initial wettability of the rock sample is oil-wet, with measured contact angle varying from 117º to 155º (average: 133.0º±13.5º). For seawater injection (SW + SW), the contact angle remains almost constant throughout the process. The injection of NaCl LSW alters the rock wettability towards slightly less oil-wet (SW + NaCl, NaCl + NaCl) and use of $CaCl_2$ (SW + $CaCl_2$, $CaCl_2$ + $CaCl_2$) alters the wettability towards more oil-wet. This observation agrees with that in the water-wet samples where NaCl promotes water-wetness and $CaCl_2$ promotes oil-wetness.

Generally, the configuration of water on rock mineral surfaces exist in two ways: (1) pendular-ring on contact points of grains; and (2) thin film on the mineral surfaces [50]. In this study, the oil drop is introduced after formation water and is kept attached to the surface throughout the experiment. Therefore, the model proposed is as shown in Figure 5, where a thin water film is formed between the rock and oil drop. A similar model was also proposed by Lee et al. [51]. They manufactured sand/clay like silica particles using simple anionic surface similar to sand grain and measured the thickness of this water film to be roughly 9-15 nm. According to their measurements on the simple wet system (fabricated simple anionic surface, similar to a sand grain) [51], the thickness of the water film on the silica/clay (sandstone-like) surface is thicker in brines with lower salinities (except for pure water). Therefore, in a system where the substrate is initially oil-wet, in order to alter the wettability from oil-wet to intermediate-wet or water-wet, a thicker water film along the pore wall is needed.

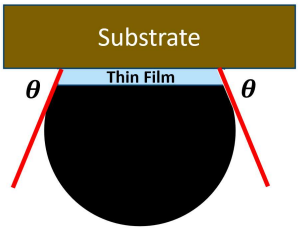

Fig. 5 A proposed model with water thin film forming between the rock/brine and oil/brine interface (Adapted from Lee et al. [51]).

Based on the results from Figure 3 and Figure 4, it is observed that the use of monovalent cations as injection brine alters the wettability towards more water-wet, which agrees with the finding from Xie et al. [52] that monovalent cations (Na^+) give rise to positive disjoining pressure; however, divalent cations (Ca^{2+}) lead to negative disjoining pressure at the same concentration. Negative disjoining pressure between rock surface and oil droplet indicates the attractive force is dominant; thus, more oil-wet is expected for the rock surface. On the other hand, positive disjoining pressure suggests the repulsive force between the rock surface and oil droplet, leading to more water-wet.

4.2 Effect of CO_2

The wettability changes caused by CO_2 after seawater injection and LSWI (NaCl or $CaCl_2$) are investigated by comparing the contact angle changes in scenarios with CO_2 (#4 and #6) and without CO_2 (#2 and #3). Contact angle changes during cycle 2 – 4 are studied. For LSWI (#2 and #3), cycle 2-4 are injection of LSW. For CO_2 + LSW (#4 and #6), cycle 2 is injection of CO_2, cycle 3-4 are injection of LSW. To calculate the changes, $\theta_{initial}$ in Eq. (1) is not the initial value in cycle 1, but the equilibrium contact angle measured after cycle 1 ($\theta_{cycle\ 1,eq}$). Hence, Eq. (4) is used to calculate contact angle changes ($\Delta\theta$) and uncertainty is calculated according to Eq. (2).

$$\Delta\theta\ [\%] = \left(\theta - \theta_{cycle\ 1,eq}\right)/\theta_{cycle\ 1,eq} \times 100 \quad (4)$$

Based on this, all the scenarios investigated in this section will start from the same point in cycle 2 with respect to contact angle change.

Figures 6 and 7 show the results of LSWI and CO_2 + LSWI after seawater injection in water-wet and oil-wet samples respectively. When comparing scenario #2 (SW + LSW) and #4 (SW + CO_2 + LSW), the addition of CO_2 after seawater promotes water-wetness for both water-wet and oil-wet samples. After CO_2 injection, further injection of $CaCl_2$ changes the wettability towards more oil-wet, and the injection of NaCl changes further more towards water-wet.

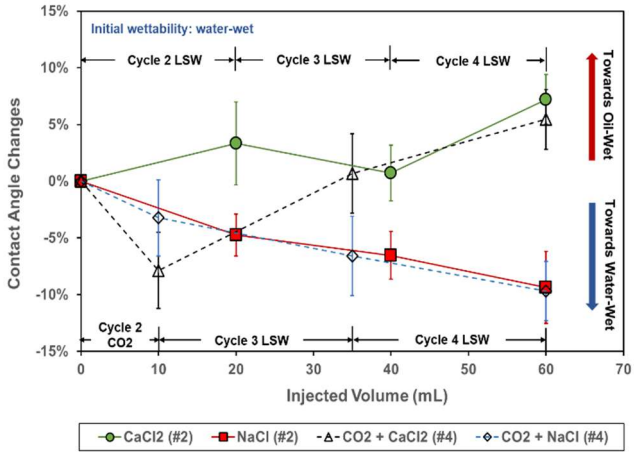

Fig. 6 Comparison of contact angle changes during LSWI and CO_2 + LSWI in water-wet sandstone after 1st cycle of seawater injection (scenario #2 and #4).

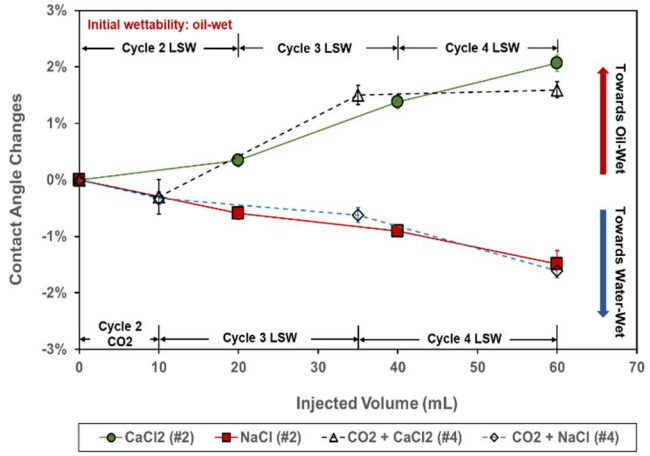

Fig. 7 Comparison of contact angle changes during LSWI and CO_2 + LSWI in oil-wet sandstone after 1st cycle of seawater injection (scenario #2 and #4).

The contact angle changes of LSWI (scenario #3) and CO_2 + LSWI (scenario #6) after LSWI in cycle 1 are shown in Figure 8 and Figure 9. Injection of LSW in cycle 2-4 has no significant impact on contact angle after the 1st cycle of LSWI. However, with the injection of CO_2 in cycle 2 and NaCl in cycle 3-4, CO_2 + NaCl alters wettability towards more water-wet in both water-wet and oil-wet samples (Figure 8 and Figure 9). For scenario #6 (CO_2 + $CaCl_2$), CO_2 alters wettability towards more water-wet, whereas further injection of $CaCl_2$ changes the wettability to more oil-wet.

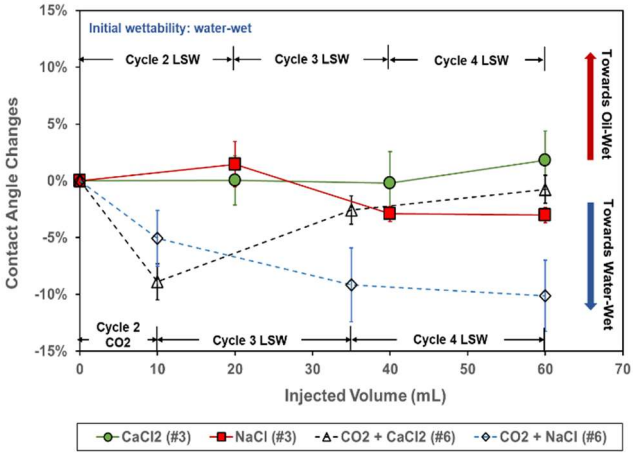

Fig. 8 Comparison of contact angle changes during LSWI and CO_2 + LSWI in water-wet sandstone after 1st cycle of LSWI (scenario #3 and #6).

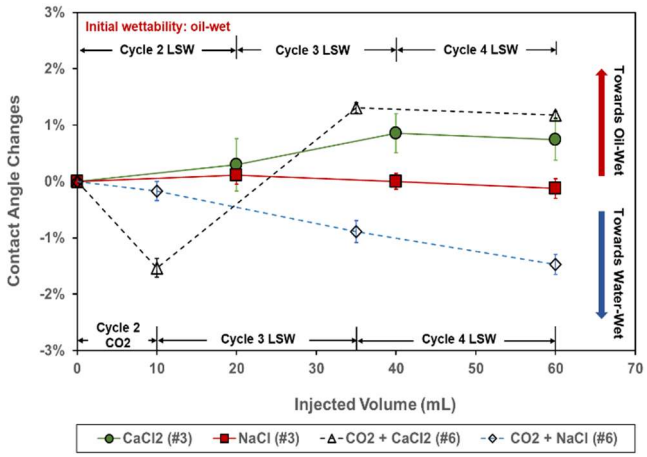

Fig. 9 Comparison of contact angle changes during LSWI and CO_2 + LSWI in oil-wet sandstone after 1st cycle of LSWI (scenario #3 and #6).

It is also observed from Figure 8 and 9 that CO_2 injected after $CaCl_2$ low salinity water alters wettability towards more water-wet compared to that injected after NaCl low salinity water. As suggested by Lager et al. [53], it is possible that divalent cations are exchanged for monovalent cations during LSWI. Therefore, in our case, more Ca^{2+} on the rock surface is expected in scenario #6 with $CaCl_2$.

When CO_2 is in contact with water, it first dissolves according to reaction (5):

$$CO_2(g) \rightleftharpoons CO_2(aq) \quad (5)$$

At room temperature, solubility of $CO_2(g)$ is 0.034 mol/L. Subsequently, reaction (6) takes place to form H_2CO_3. This reaction is kinetically slow and only a small fraction (0.2 – 1.0%) of dissolved CO_2, $CO_2(aq)$, is converted to H_2CO_3.

$$CO_2(aq) + H_2O \rightleftharpoons H_2CO_3(aq) \quad (6)$$

However, this carbonic acid dissociates very rapidly at ambient conditions to bicarbonate [54], as shown in reaction (7). The bicarbonate electrolyte in the solution can also form CO_3^{2-} as shown by reaction (8).

$$H_2CO_3(aq) \rightleftharpoons HCO_3^- + H^+ \quad (7)$$

$$HCO_3^- \rightleftharpoons CO_3^{2-} + H^+ \quad (8)$$

With the injection of CO_2, some of the produced CO_3^{2-} would potentially react with the existing Ca^{2+} ions, forming $CaCO_3$, which results in equation (8) to move to the right direction, leading to slight increase in H^+. Based on the selectivity of cation affinity to negatively charged surfaces from Velde [55], as shown below, the proton H^+ has the strongest affinity to be adsorbed onto a negatively charged surface.

$$Li^+ < Na^+ < K^+ < Mg^{2+} < Ca^{2+} < H^+$$

Therefore, the generated H^+ is likely to replace the pre-attached divalent cations, resulting in more water-wetness. In this way, the injection of CO_2 after $CaCl_2$ low salinity water alters wettability towards more water-wet compared to injection of CO_2 after NaCl low salinity water.

4.3 Surfactant-Like Behavior of Oil Drops

During the injection of LSW and a combination of CO_2 and LSW in the water-wet and oil-wet samples, a surfactant-like deformation process of the oil drop is constantly observed when the initial equilibrium of the system is disturbed. The oil drop deformation with and without CO_2 is discussed respectively in the subsections.

4.3.1 Deformation in the absence of CO_2

Figure 10 and Figure 11 illustrate the deformation process during the injection of NaCl LSW in water-wet and $CaCl_2$ LSW in oil-wet sandstones, respectively. For NaCl LSWI in water-wet sample, the contact angle varies from water-wet to intermediate-wet and then back to more water-wet while reaching equilibrium. For $CaCl_2$ LSWI in oil-wet sample, contact angle changes from oil-wet to intermediate-wet and then back to more oil-wet in the end.

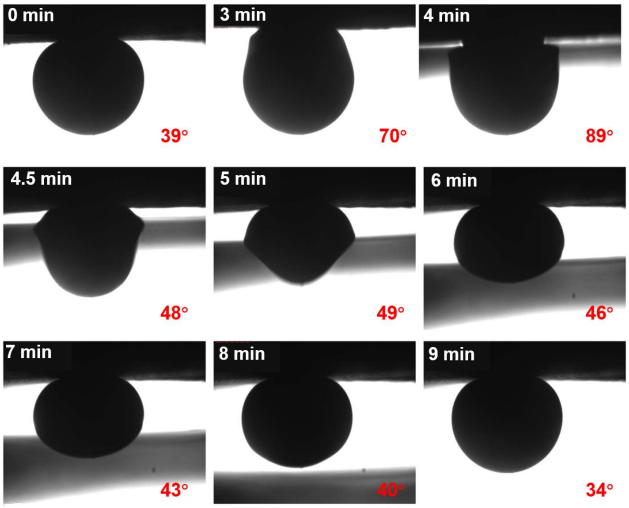

Fig. 10 Oil drop deformation process during NaCl LSWI in water-wet sandstone (scenario #3).

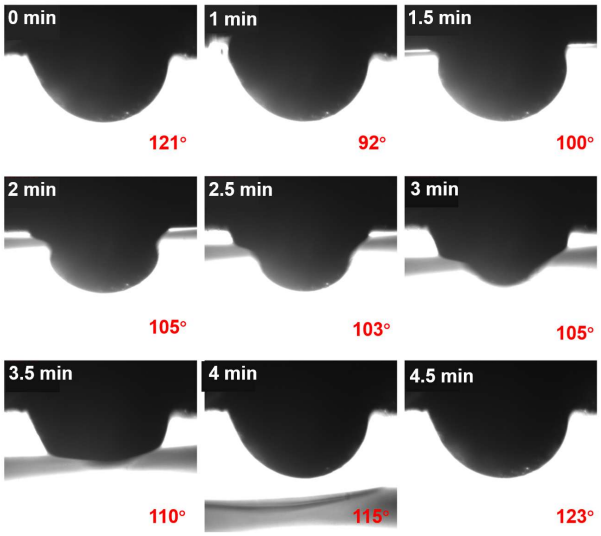

Fig. 11 Oil drop deformation process in time during $CaCl_2$ LSWI in an oil-wet sandstone system (scenario #3).

Based on Figures 10 and 11, the deformation process during LSWI resembles a surfactant-like behaviour. The potential removal of the droplet exhibits a "necking" or emulsification mechanism. One mechanism for LSWI proposed by McGuire et al. [56] suggests that the changes in wettability during low salinity water injection appear to be similar to the observations from alkaline and surfactant flooding. In this study, the interactions between the oil drop and injection fluids are more dominant due to the presence of just one oil drop. As listed in Table 1, the pH of the injection fluids is higher compared to that of the initial formation water. During the injection of low salinity water, in-situ "surfactants" are generated, as shown in Eq. (9), when the oil drop is in contact with the elevated pH fluid near the rock and oil surfaces. This improves oil recovery [56]. In this way, low salinity water injection is similar to micellar or surfactant flooding.

$$(R_1COO)_3R_2 + 3NaOH \leftrightarrow 3(R_1COONa) + R_2(OH)_3 \quad (9)$$

where R_1 and R_2 represent the R group, which consists of a group of carbon and hydrogen atoms.

According to the study of oil removal from soil surfaces by Miller and Raney [57], two approaches are proposed as mechanisms for oil removal from hydrophobic surfaces using surfactants: (1) roll-up resulting from wetting; and (2) emulsification resulting from reduction in interfacial tension (Figure 12).

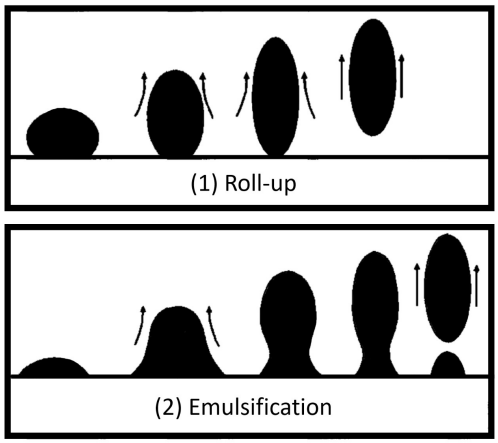

Fig. 12 Mechanisms of oil removal from surface by (1) roll-up and (2) emulsification (adapted from Miller and Raney [57]).

4.3.2 Deformation with CO_2 present

The top two pictures shown in Figure 13 are the oil drop deformation during injection of CO_2 + $CaCl_2$, (scenario #4) and the bottom two pictures are during $CaCl_2$ LSWI (scenario #2). These two deformation processes resemble the two approaches in Figure 12. Without addition of CO_2, the detachment of the oil drop is a saponification or emulsification process. However, the roll-up process is expected with CO_2 due to the geochemical reactions that change the wetting state of the contact point on the rock surface.

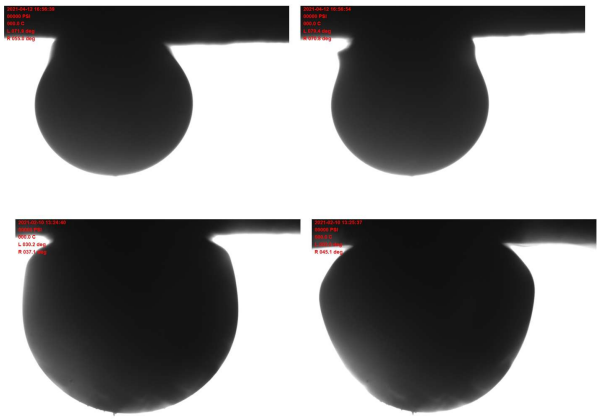

Fig. 13 Comparison of oil drop deformation process: top (scenario #4): during CO_2 and $CaCl_2$ injection (roll-up); bottom (scenario #2): during $CaCl_2$ injection (emulsification) after seawater injection in water-wet sandstone.

4.4 Effect of Injection Scheme

The impact of different injection schemes with respect to CO_2 is explored by comparing the scenarios of SW + CO_2 + LSW (#4) and SW + LSWAG (#5), and scenarios of LSW + CO_2 + LSW (#6) and LSW + LSWAG (#7).

Contact angle changes of scenario #4 and #5 are shown in Figure 14 and Figure 15. It is observed that after 1st cycle of seawater injection, further injection of CO_2 + $CaCl_2$ alters wettability in the direction of more oil-wet, however, CO_2/$CaCl_2$ WAG injection alters rock wettability towards more water-wet. Injection schemes of CO_2 + NaCl and CO_2/NaCl WAG both change the rock wettability to more water-wet, whereas changes are more significant for CO_2 + NaCl. The wettability changes by CO_2/LSWAG processes (for both NaCl and $CaCl_2$) are not as significant as CO_2 + LSW injection when implemented after seawater injection (Figure 14 and Figure 15).

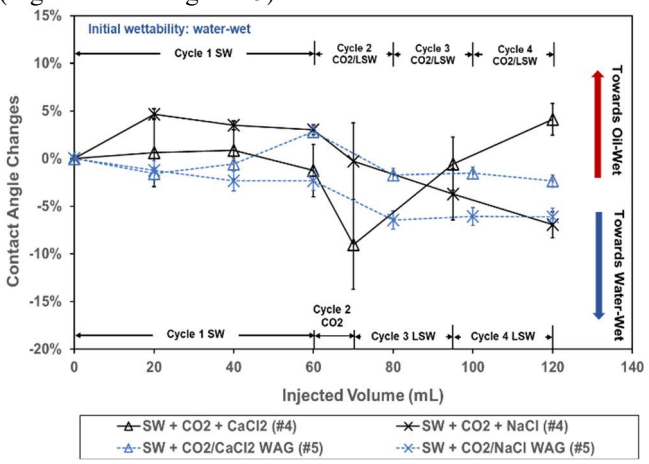

Fig. 14 Comparison of contact angle changes during SW + CO_2 + LSWI and SW + CO_2/LS WAG injection in water-wet sandstone (scenario #4 and #5).

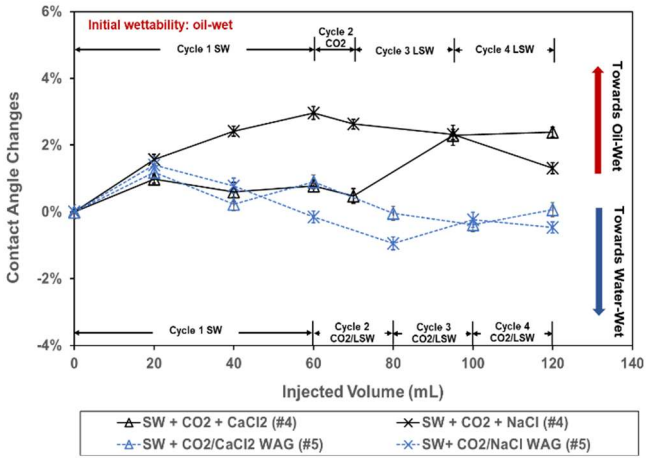

Fig. 15 Comparison of contact angle changes during SW + CO_2 + LSWI and SW + CO_2/LSWAG injection in oil-wet sandstone (scenario #4 and #5), error bars are too small to be seen.

Figure 16 and Figure 17 show the comparison between #6 (LSW + CO_2 + LSW) and #7 (LSW + CO_2/LSWAG) in water-wet and oil-wet samples. The results in the figures show that the addition of CO_2 has a minor effect on the wettability for the CO_2/NaCl WAG process. When comparing CO_2 + $CaCl_2$ with CO_2/$CaCl_2$ WAG injection in both water-wet and oil-wet samples, the trend for wettability change is different. For the scheme of CO_2 + $CaCl_2$ injection, the addition of CO_2 promotes water-wetness of the rock, and the chasing $CaCl_2$ low salinity water changes the wettability back to more oil-wet. However, in the CO_2/$CaCl_2$ WAG process, the wettability is altered towards more water-wet.

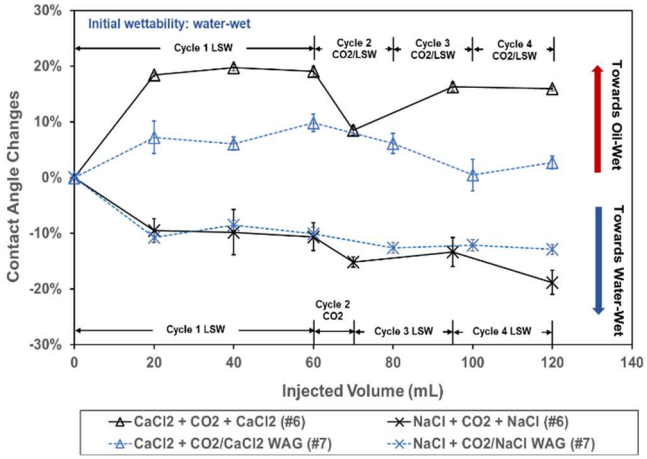

Fig. 16 Comparison of contact angle changes during LSWI, CO_2 and LSWI, and CO_2 LSWAG injection in water-wet sandstone (scenario #6 and #7), some error bars are too small to be seen.

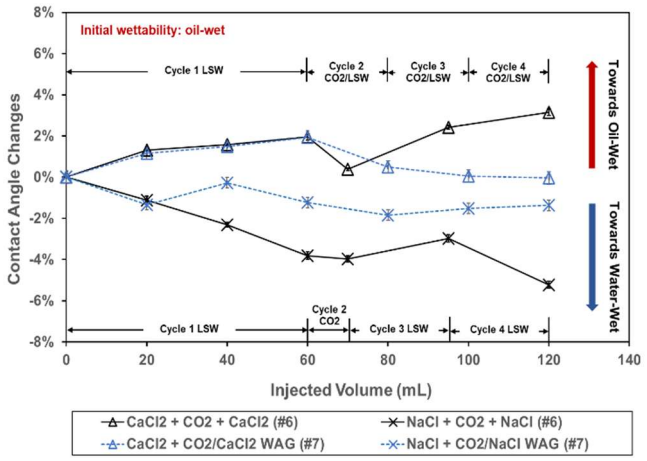

Fig. 17 Comparison of contact angle changes during LSWI, CO_2 and LSWI, and CO_2 LSWAG injection in oil-wet sandstone (scenario #6 and #7), error bars are too small to be seen.

The WAG process of CO_2 and $CaCl_2$ low salinity water leads to wettability alteration to slightly water-wet. With respect to the scenario of CO_2 + $CaCl_2$ (#6), even though CO_2 changes wettability to be more water-wet, the generated H^+ is not sufficient. Thus, subsequent injection of $CaCl_2$ replaces the monovalent cations and alters the rock wettability towards more oil-wet.

Summarising, if NaCl LSW is used, the continuous CO_2 + NaCl injection scheme is more efficient than WAG cycle of CO_2/NaCl in achieving a more water-wet condition of sandstone. However, if $CaCl_2$ LSW is used, WAG cycle of CO_2/$CaCl_2$ can alter the rock wettability to be more water-wet compared to continuous CO_2 + $CaCl_2$ injection.

5 Conclusion

In this study, a displacement method for measuring contact angle changes during the process of seawater injection, LSWI, CO_2 and LSWI, and CO_2 LSWAG injection has been conducted. Seawater, low salinity water with only monovalent and divalent cations are selected as the injection aqueous phases. The effect of these ions, oil drop deformation process, and the effect of CO_2 and injection scheme have been investigated.

1. It is found that for our Berea sandstone with an initial wettability of either water-wet and oil-wet[1], the injection of 2000 ppm NaCl water alters the wettability towards slightly water-wet, and the injection of 2000 ppm $CaCl_2$ alters the wettability towards slightly oil-wet. Low salinity water with divalent cation could increase the attraction forces between the oil/rock and oil/brine interfaces, promoting oil-wetness. However, low salinity with monovalent cation reduces the attraction forces, i.e., repulsive force increases, therefore, resulting in more water-wet.
2. The deformation process during LSWI resembles the process of oil removal using surfactant. This "surfactant-like" behaviour lowers the interfacial tension and contributes to increased oil recovery. As CO_2 is introduced, due to the acidic effect of CO_2, it acts to wet the rock surface, leading to a more water-wet state. Therefore, the oil removal or oil drop deformation resembles the "roll-up" oil removal process.
3. The injection of CO_2 promotes water-wetness and geochemical reactions between oil and brine. In the WAG process, more interactions between injection brine, CO_2 and pre-existing brine are expected, and this leads to different wettability alteration trend compared to CO_2 + LSWI. When NaCl LSW is used, continuous CO_2 + NaCl injection scheme is more efficient than WAG cycle of CO_2/NaCl in wettability alteration towards more water-wet. However, with $CaCl_2$ LSW, WAG cycle of CO_2/$CaCl_2$ can alter the rock wettability to be more water-wet compared to continuous CO_2 + $CaCl_2$ injection.

6 Future Work

In this study, all the measurements are conducted at ambient condition. The effect of temperature and pressure is not considered. As the temperature and pressure exceeds the critical point for CO_2, the state of CO_2 will become supercritical, with properties midway between a gas and a liquid. Therefore, in order to better understand the wettability alterations with supercritical CO_2, more research with respect to elevated temperature and pressure should be carried out in the future. If wettability alteration is considered as the main mechanism for LSWI or CO_2 LSWAG injection, this displacement contact angle measurement which mimics the real reservoir displacement process could be used as a preliminary screening for brine concentration and composition, as well as injection schemes. However, to achieve a systematic evaluation process, more experimental data with respect to temperature and pressure are required.

[1] Note: wettability was inferred from the contact angle and was not independently verified by measurements like USBM or Amott.

7 Acknowledgements

The authors would like to thank the Hibernia Management and Development Company (HMDC), Chevron Canada Ltd, Petroleum Research Newfoundland and Labrador (PRNL), the Natural Sciences and Engineering Research Council of Canada (NSERC), the Province of Newfoundland and Labrador, and Mitacs for financial support. We thank our colleagues in the Hibernia EOR Research Group for their technical support.

References

1. N. Morrow, and J. Buckley, Improved oil recovery by low-salinity waterflooding. Journal of petroleum Technology, **63**(05), pp.106-112, SPE-129421-JPT. (2011).
2. K.J. Webb, C.A. Black, H. Al-Ajeel, Low salinity oil recovery-log-inject-log. In SPE/DOE Symposium on Improved Oil Recovery, SPE-89379-MS. (2004).
3. K.J. Webb, C.J.J Black, I.J. Edmonds, Low salinity oil recovery – The role of reservoir condition corefloods. In IOR 2005-13th European Symposium on Improved Oil Recovery (pp. cp-12). European Association of Geoscientists & Engineers. (2005).
4. L. Moghadasi, P. Pisicchio, M. Bartosek, E. Braccalenti, P. Albonico, I. Moroni, R. Veschi, F. Masserano, S. Scagliotti, L. Del Gaudio, M. De Simoni, Laboratory investigation on synergy effect of low salinity-polymer water injection on sandstone porous media. In Offshore Mediterranean Conference and Exhibition, OMC-2019-0868. (2019).
5. E. Alagic, A. Skauge, Combined low salinity brine injection and surfactant flooding in mixedwet sandstone cores. Energy & fuels, **24**(6), pp.3551-3559. (2010).
6. T.W. Teklu, W. Alameri, H. Kazemi, R.M. Graves, A.M. AlSumaiti, Low salinity water – Surfactant – CO2 EOR. Petroleum, **3**(3), pp.309-320. (2017).
7. M.T. Al-Murayri, H.E. Al-Mayyan, K. Moudi, F. Al-Ajmi, D. Pitts, M.J. Wyatt, K.French, J. Surtek, E. Dean, Chemical EOR Economic Evaluation in a Low Oil Price Environment: Sabriyah Lower Burgan Reservoir Case Study. In SPE EOR Conference at Oil and Gas West Asia, SPE-190337-MS. (2018).
8. H. Muriel, S. Ma, S.J.D. Sofla, L.A. James, Technical and Economical Screening of Chemical EOR Methods for the Offshore. In Offshore Technology Conference, OTC-30740-MS. (2020).
9. H. Jiang, L. Nuryaningsih, H. Adidharma, The effect of salinity of injection brine on water alternating gas performance in tertiary miscible carbon dioxide flooding: experimental study. In SPE Western Regional Meeting, SPE-132369-MS. (2010).
10. R. Ramanathan, A.M. Shehata, H.A. Nasr-El-Din, Water Alternating CO2 Injection Process-Does Modifying the Salinity of Injected Brine Improve Oil Recovery?. In OTC Brasil, OTC-26253-MS. (2015).
11. A.A. AlQuraishi, A.M.Amao, N.I. Al-Zahrani, M.T. AlQarni, S.A. AlShamrani, Low salinity water and CO2 miscible flooding in Berea and Bentheimer sandstones. Journal of King Saud University-Engineering Sciences, **31**(3), pp.286-295. (2019).
12. N.R. Morrow, G.Q. Tang, M. Valat, X. Xie, Prospects of improved oil recovery related to wettability and brine composition. Journal of Petroleum science and Engineering, **20**(3-4), pp.267-276. (1998).
13. N.R. Morrow, Wettability and its effect on oil recovery. Journal of petroleum technology, **42**(12), pp.1476-1484. (1990).
14. H. Al-Abri, P. Pourafshary, N. Mosavat, H. Al Hadhrami, A study of the performance of the LSWA CO2 EOR technique on improvement of oil recovery in sandstones. Petroleum, **5**(1), pp.58-66. (2019).
15. T.W. Teklu, W. Alameri, R.M. Graves, H Kazemi, A.M. AlSumaiti, Low-salinity water-alternating-CO2 flooding enhanced oil recovery: theory and experiments. In Abu Dhabi International Petroleum Exhibition and Conference, SPE-171767-MS. (2014).
16. R.M. Enick, S.M. Klara, CO2 solubility in water and brine under reservoir conditions. Chemical Engineering Communications, **90**(1), pp.23-33. (1990).
17. Y.K. Li, L.X.Nghiem, Phase equilibria of oil, gas and water/brine mixtures from a cubic equation of state and Henry's law. The Canadian Journal of Chemical Engineering, **64**(3), pp.486-496. (1986).
18. K.R Chaturvedi, D. Ravilla, W. Kaleem, P. Jadhawar, T. Sharma, Impact of low salinity water injection on CO2 storage and oil Recovery for improved CO2 utilization. Chemical Engineering Science, 229, p.116127. (2021).
19. H. Zolfaghari, A. Zebarjadi, O. Shahrokhi, M.H. Ghazanfari, An experimental study of CO2-low salinity water alternating gas injection in sandstone heavy oil reservoirs. Iranian Journal of Oil & Gas Science and Technology, **2**(3), pp.37-47. (2013).
20. H.N. Al-Saedi, S.K. Al-Jaberi, R.E.Flori, W. Al-Bazzaz, Y. Long, A new design of low salinity-CO2-different chemical matters. In Abu Dhabi International Petroleum Exhibition & Conference, SPE-197118-MS. (2019).
21. H.N. Al-Saedi, R.E. Flori, Novel coupling smart water-CO2 flooding for sandstone reservoirs. Petrophysics-The SPWLA Journal of Formation Evaluation and Reservoir Description, **60**(04), pp.525-535. (2019).
22. H.N. Al-Saedi, Y. Long, R.E. Flori, B. Bai, Coupling smart seawater flooding and CO2 flooding for sandstone reservoirs: smart seawater alternating CO2 flooding (SMSW-AGF). Energy & Fuels, **33**(10), pp.9644-9653. (2019).
23. L.W. Holm, V.A .Josendal, Mechanisms of oil displacement by carbon dioxide. Journal of petroleum Technology, **26**(12), pp.1427-1438. (1974).
24. M.S.A. Perera, R.P. Gamage, T.D. Rathnaweera, A.S. Ranathunga, A. Koay, X. Choi, A review of CO2-enhanced oil recovery with a simulated sensitivity analysis. Energies, **9**(7), p.481. (2016).

25. C. Drummond, J. Israelachvili, Surface forces and wettability. Journal of Petroleum Science and Engineering, **33**(1-3), pp.123-133. (2002).
26. J.J. Sheng, Critical review of low-salinity waterflooding. Journal of Petroleum Science and Engineering, **120**, pp.216-224. (2014).
27. P.P. Jadhunandan, N.R. Morrow, Effect of wettability on waterflood recovery for crude-oil/brine/rock systems. SPE reservoir engineering, **10**(01), pp.40-46, SPE-22597-PA. (1995).
28. A. Lager, K.J. Webb, C.J.J. Black, Impact of brine chemistry on oil recovery. In IOR 2007-14th European symposium on improved oil recovery (pp. cp-24). European Associ. of Geoscientists & Engineers. (2007).
29. D.J. Ligthelm, J. Gronsveld, J. Hofman, N. Brussee, F. Marcelis, H. van der Linde, Novel waterflooding strategy by manipulation of injection brine composition. In EUROPEC/EAGE conference and exhibition, SPE-119835-MS. (2009).
30. R.T. Johansen, H.N. Dunning, Relative wetting tendencies of crude oils by capillarimetric method, **5752**. US Department of the Interior, Bureau of Mines. (1961).
31. J.W. Graham, J.G. Richardson, Theory and application of imbibition phenomena in recovery of oil. Journal of Petroleum Technology, **11**(02), pp.65-69. (1959).
32. N.R. Morrow, G. Mason, Recovery of oil by spontaneous imbibition. Current Opinion in Colloid & Interface Science, **6**(4), pp.321-337. (2001).
33. L.E. Treiber, W.W. Owens, A laboratory evaluation of the wettability of fifty oil-producing reservoirs. Society of petroleum engineers journal, **12**(06), pp.531-540, SPE-3526-PA. (1972).
34. J.P. Batycky, F.G. McCaffery, P.K. Hodgins, D.B. Fisher, Interpreting relative permeability and wettability from unsteady-state displacement measurements. Society of Petroleum Engineers Journal, **21**(03), pp.296-308, SPE-9403-PA. (1981).
35. A.B.D. Cassie, S. Baxter, Wettability of porous surfaces. Transactions of the Faraday society, **40**, pp.546-551. (1944).
36. N. Siemons, H. Bruining, H. Castelijns, K.H. Wolf, Pressure dependence of the contact angle in a CO2 – H2O – coal system. Journal of colloid and interface science, **297**(2), pp.755-761. (2006).
37. E. Sripal, L.A. James, Application of an optimization method for the restoration of core samples for SCAL experiments. Petrophysics-The SPWLA Journal of Formation Evaluation and Reservoir Description, **59**(01), pp.72-81. (2018).
38. E. Sripal, D. Grant, L. James, Application of SEM Imaging and MLA Mapping Method as a Tool for Wettability Restoration in Reservoir Core Samples for SCAL Experiments. Minerals, **11**(3), p.285. (2021).
39. W. Anderson, Wettability literature survey-part 2: Wettability measurement. Journal of petroleum technology, **38**(11), pp.1246-1262. (1986).
40. M. Arif, S.A. Abu-Khamsin, S. Iglauer, Wettability of rock/CO_2/brine and rock/oil/CO_2-enriched-brine systems: Critical parametric analysis and future outlook. Advances in colloid and interface science, **268**, pp.91-113. (2019).
41. N.S. Kaveh, E.S.J. Rudolph, P. Van Hemert, W.R.Rossen, K.H. Wolf, Wettability evaluation of a CO2/water/bentheimer sandstone system: contact angle, dissolution, and bubble size. Energy & Fuels, **28**(6), pp.4002-4020. (2014).
42. S.J.D. Sofla, L.A. James, Y. Zhang, Toward a mechanistic understanding of wettability alteration in reservoir rocks using silica nanoparticles. In E3S Web of Conferences, **89**, p. 03004. EDP Sciences. (2019).
43. P.T. Jaeger, M.B. Alotaibi, H.A. Nasr-El-Din, Influence of compressed carbon dioxide on the capillarity of the gas− crude oil− reservoir water system. Journal of Chemical & Engineering Data, **55**(11), pp.5246-5251. (2010).
44. A. Ameri, N.S. Kaveh, E.S.J. Rudolph, K.H. Wolf, R. Farajzadeh, J. Bruining, Investigation on interfacial interactions among crude oil – brine – sandstone rock – CO2 by contact angle measurements. Energy & fuels, **27**(2), pp.1015-1025. (2013).
45. D.N. Espinoza, J.C. Santamarina, Water - CO2 - mineral systems: Interfacial tension, contact angle, and diffusion — Implications to CO2 geological storage. Water resources research, **46**(7). (2010).
46. M. Seyyedi, M. Sohrabi, A. Farzaneh, Investigation of rock wettability alteration by carbonated water through contact angle measurements. Energy & Fuels, **29**(9), pp.5544-5553. (2015).
47. A.B. Dixit, S.R. McDougall, K.S. Sorbie, J.S. Buckley, Pore scale modelling of wettability effects and their influence on oil recovery. In SPE/DOE Improved Oil Recovery Symposium, SPE-35451-MS. (1996).
48. S.J. Kline, F.A. McClintock, Describing uncertainties in single sample experiments. Mech. Engineering, 75, pp.3-8. (1953).
49. S. Li, M. Liu, D. Hanaor, Y. Gan, Dynamics of viscous entrapped saturated zones in partially wetted porous media. Transport in Porous Media, **125**(2), pp.193-210. (2018).
50. H. Ding, S. Rahman, Experimental and theoretical study of wettability alteration during low salinity water flooding-an state of the art review. Colloids and Surfaces A: Physicochemical and Engineering Aspects, **520**, pp.622-639. (2017).
51. S.Y. Lee, K.J. Webb, I.R. Collins, A. Lager, S.M. Clarke, M. O'Sullivan, A.F. Routh, X. Wang, Low salinity oil recovery – Increasing understanding of the underlying mechanisms. In SPE Improved Oil Recovery Symposium. SPE-129722-MS. (2010).
52. Q. Xie, A. Saeedi, E. Pooryousefy, Y. Liu, Extended DLVO-based estimates of surface force in low salinity water flooding. Journal of Molecular Liquids, **221**, pp.658-665. (2016).

53. A. Lager, K.J. Webb, C.J.J. Black, M. Singleton, K.S. Sorbie, Low salinity oil recovery-an experimental investigation1. Petrophysics-The SPWLA Journal of Formation Evaluation and Res. Descrip. **49**(01). (2008).
54. H. Wang, J. Zeuschner, M. Eremets, I. Troyan, J. Willams, Stable solid and aqueous H2CO3 from CO2 and H2O at high pressure and high temperature. Scientific Reports, **6**(1), pp.1-8. (2016).
55. B. Velde, *Origin and mineralogy of clays: clays and the environment*. Springer Sci. & Business Media. (2013)
56. P.L McGuire, J.R. Chatham, F.K. Paskvan, D.M. Sommer, F.H. Carini, Low salinity oil recovery: An exciting new EOR opportunity for Alaska's North Slope. SPE-93903-MS. (2005).
57. C.A. Miller, K.H. Raney, Solubilization - emulsification mechanisms of detergency. Colloids and Surfaces A: Physicochemical and Engineering Aspects, **74**(2-3), pp.169-215. (1993).